Materials & Design 254 (2025) 114047

Contents lists available at ScienceDirect

Materials & Design

journal homepage: www.elsevier.com/locate/matdes

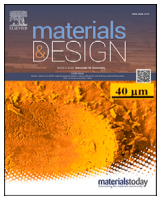

Exploring elastic properties of molecular crystals with universal machine learning interatomic potentials

Anastasiia Kholtobina, Ivor Lončarić *

Ruđer Bošković Institute, Bijenička 54, Zagreb, Croatia

ARTICLE INFO

Dataset link: https://doi.org/10.5281/zenodo.15225984

ABSTRACT

We benchmarked existing and newly trained universal machine learning interatomic potentials for modeling molecular crystals, particularly their elastic properties. We found that potentials trained on the SPICE dataset provide reasonable predictions of the elastic properties of molecular crystals that are as good as predictions made using density functional theory-based methods. Still, the uncertainty of predictions and difference to experimental values is relatively high (larger than 5 GPa for Young's modulus). We have performed a high-throughput study of the elastic properties of molecular crystals. We have found that some of the molecular crystals show negative linear compressibility and validated our results using density functional theory.

1. Introduction

Universal machine learning interatomic potentials (UMLIPs), also called global potentials or foundational models, are becoming new tools of choice for screening and discovering materials with useful properties [1,2]. Their applicability and success to model different material properties is a very active area of research, as well as the competition to build the most accurate model. For example, Matbench Discovery presents leaderboard which ranks UMLIPs on a task of simulating high-throughput discovery of new stable inorganic crystals predicting some of their properties [3]. The most important factor for the accuracy of UMLIP is the size of the dataset and its coverage of the configurational space.

In this sense, molecular crystals are uniquely difficult for the current UMLIPs as they are commonly trained on density functional theory (DFT) databases of either inorganic crystals with rather small unit cells or isolated organic molecules. Molecular crystals, on the other hand, usually have large unit cells and large DFT databases that include them do not exist. Still, molecular crystals play an important role in areas ranging from mechanics and electronics to medicine and pharmacy and are prospective candidates in future dynamic active materials such as medical devices, actuators and materials for electronics [4,5]. Therefore, it is very important to understand the validity of current UMLIPs for modeling molecular crystals.

Theoretical methods for modeling molecular crystals are usually benchmarked on the X23b benchmark set [6] as an experimental reference for the lattice energies and structures of 23 well-characterized systems. Benchmarking the first derivatives of the potential energy surface and higher derivatives is a stricter and more robust metric for measuring the utility and the physical accuracy of UMLIPs. To the best of our knowledge, the most extensive such experimental reference for molecular crystals is the database of 44 full elastic tensors by Spackman et al. [7]. Accurate estimation of elastic constant tensors can be obtained using density functional theory (DFT) with dispersion correction (DFT-D) [8–10]. Spackman et al. [7] also utilized the corrected small basis set Hartree–Fock method (S-HF-3c) as a cheaper alternative compared to DFT-D. Since DFT simulations require significant computational resources, the UMLIPs should enable the calculations on a large scale. Recently conducted research revealed that the accuracy of some MLIPs for elastic tensors can be closer to DFT-D than S-HF-3c [11].

In this article, we first use the existing and newly created UMLIPs trained on the existing large databases of small (inorganic) crystals as well as molecules (and their dimers) to benchmark their performance on the X23b and elastic tensors benchmark dataset. Best-performing models are then used for the high-throughput screening of elastic properties of molecular materials. In addition to the map of elastic properties of molecular crystals, we have found some molecular crystals with fascinating properties, such as negative linear compressibility. We have validated our predictions with DFT-D simulations.

* Corresponding author.
E-mail address: ivor.loncaric@gmail.com (I. Lončarić).

https://doi.org/10.1016/j.matdes.2025.114047
Received 27 January 2025; Received in revised form 29 April 2025; Accepted 3 May 2025
Available online 8 May 2025

2. Methodology

2.1. Models

Several existing, as well as a few newly trained UMLIPs are used in this work. Of existing UMLIPs, we start with those trained mostly on inorganic crystals based on DFT-PBE(+U) calculations. MACE-MP-0 [12] is trained with MACE [13] architecture on MPtrj dataset [14]. We use only the "large" model size coupled with D3 correction [15]. MatterSim (MatterSim-v1.0.0-5M) [16] is trained with M3GNet [17] architecture on MatterSim data [16]. We have added D4 correction [18] on top of this UMLIP. Orb-d3-v2 [19] was trained with graph network simulator [20] augmented with a smoothed graph attention mechanism on MPtrj+Alexandria [21,22] dataset. OMAT24eqV2_86M [23] was trained with EquiformerV2 [24] architecture on OMAT24 database [23], and we have added D4 correction [18] on top of this UMLIP.

The second class of existing UMLIPs are those trained on databases composed mostly of calculations for small organic molecules. MACE-OFF23 [25] is trained with MACE [13] architecture on the SPICE 1.0 dataset [26] that provides data for small molecules, dimers, dipeptides, and solvated amino acids at the ωB97M-D3(BJ)/def2-TZVPPD level of theory. We use only the "large" model size. Nequip@ANI1x [27] is our previously trained model, trained with the Nequip architecture [28] on the ANI1x dataset [29] that is supplemented with D4 correction [18].

The only dataset that is composed of molecular crystals is the OMDB [30], and our previously trained model Nequip@OMDB [27] is trained with the Nequip architecture [28] and supplemented with D4 correction [18].

Finally, in this work, we have trained MACE@SPICE2 UMLIP, which differs from "large" MACE-OFF23 only by the updated training database SPICE 2.0 that doubled the total amount of data compared to SPICE 1.0 keeping the same level of theory. To be able to study the uncertainty of predictions we have also trained five versions of Nequip@SPICE models for which we used the SPICE 1.0 database and Nequip model training hyperparameters were the same as for Nequip@ANI1x [27]. Namely, n_{layer} and r_{cutoff} were chosen as 4 and 5 Å, respectively. Five different random seeds were used in order to obtain different UMLIPs.

2.2. Elastic constant calculations

The elastic tensor is obtained from strain-stress fit as implemented in pymatgen [31]. Each (strained) structure was relaxed until forces on atoms were smaller than 0.001 eV/Å. Temperature effects are neglected for simplicity and efficiency, but could be added in spirit of, for example, Refs. [32,33]. The elastic tensor was used to derive the material properties such as bulk modulus (K), shear modulus (G), and Young's modulus (E) (using Voigt (V), Reuss (R) and Hill (H) estimates). The arithmetic mean of the Reuss and Hill averages is a better approximation according to the literature [7] and is used in this work. Calculations of linear compressibility were performed according to expressions from Nye [34] using the ELATE tool [35].

2.3. DFT validation

The DFT validation of the elastic properties predicted by UMLIPs was performed using the same workflow as with UMLIPs. For DFT calculations, we used an all-electron electronic structure code FHI-aims [36–39] with intermediate basis set defaults and k-point grid density of at least 5 Å. For exchange-correlation functional we used PBE [40] with many-body dispersion (MBD) correction [41,42]. PBE+MBD offers accurate description of elastic properties of molecular crystals [43–46].

3. Results and discussion

Before focusing on the mechanical properties of molecular crystals, we first benchmark the accuracy of studied UMLIPs in predicting lattice energies and volumes on the well-established experimental benchmark database X23b [6]. Fig. 1 and Table 1 show the accuracy of volume predictions of studied UMLIPs. Most of UMLIPs relax crystal structures to reasonable volumes within −5% to 5% from the experimental value (corrected for temperature effects). Notable exceptions are results for CO_2 where MACE-OFF23 and Nequip@OMDB+D4, and, to a lesser extent, MatterSim+D4 predict significantly larger volumes. For this reason, in Table 1 we also list results with CO_2 excluded from the analysis. A number of UMLIPs provide better predictions than DFT with PBE-MBD, notably MACE@SPICE2, orb-d3-v2, and OMAT24eqV2_86M+D4.

Fig. 2 and Table 2 show a comparison of lattice energies calculated with UMLIPs to X23b benchmark [6]. It can be observed in Fig. 2 that most of UMLIPs provide reasonable lattice energies. However, comparing errors of UMLIPs and typical DFT approximation (PBE-MBD) one

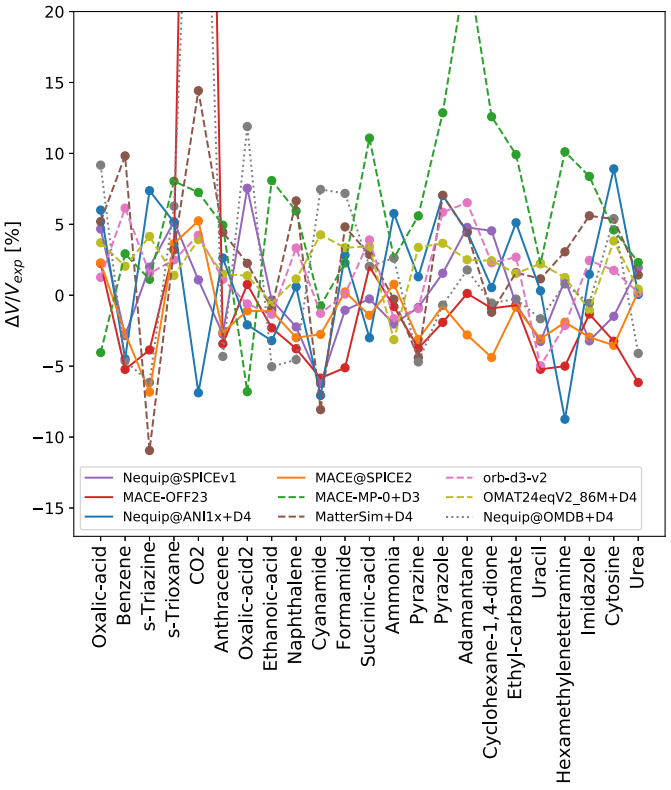

Fig. 1. Relative difference of UMLIPs predictions and experimental benchmark X23b [6] volumes. Full lines represent UMLIPs trained on molecular data, dashed lines represent UMLIPs trained on mostly inorganic data, and dotted line represents model trained on molecular crystals.

Table 1
Analysis of Mean Absolute Error (MAE, %), Mean Error (ME, %), and Standard Deviation (SD, %) of relative error of different UMLIPs predictions for unit cell volumes compared to X23b dataset [6]. Data in brackets are without CO_2.

	MAE	ME	SD
Nequip@ANI1x+D4	4.13 (4.01)	1.05 (1.41)	4.83 (4.63)
Nequip@SPICEv1	2.68 (2.75)	**0.31** (**0.28**)	3.29 (3.36)
MACE-OFF23	6.92 (3.04)	1.82 (-2.28)	19.42 (2.71)
MACE-MP-0+D3	6.87 (6.85)	5.86 (5.8)	6.15 (6.28)
MACE@SPICE2	2.49 (**2.36**)	-1.41 (-1.71)	2.6 (2.22)
MatterSim+D4	4.75 (4.31)	2.5 (1.96)	5.32 (4.77)
orb-d3-v2	2.56 (2.48)	1.43 (1.3)	2.81 (2.81)
OMAT24eqV2_86M+D4	**2.44** (2.38)	2.03 (1.95)	**1.81** (**1.81**)
Nequip@OMDB+D4	6.14 (4.17)	2.9 (0.79)	11.09 (5.09)
PBE-MBD [47,27]	5.07	5.07	2.71

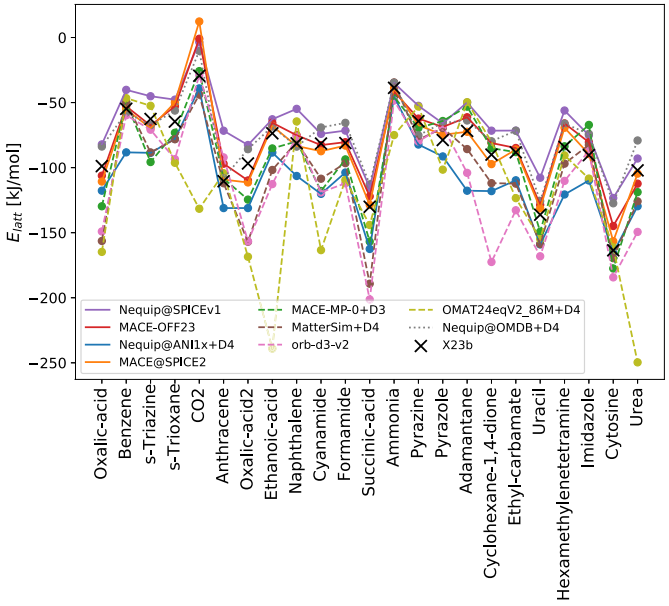

Fig. 2. Comparison of lattice energies calculated by UMLIPs to corrected experimental benchmark X23b values (black markers). Full lines represent UMLIPs trained on molecular data, dashed lines represent UMLIPs trained on mostly inorganic data, and dotted line represents model trained on molecular crystals.

Table 2
Analysis of Mean Absolute Error (MAE, kJ/mol), Mean Error (ME, kJ/mol), and Standard Deviation (SD, kJ/mol) of different UMLIPs predictions for lattice energies compared to X23b dataset [6]. Data in brackets are without CO_2.

	MAE	ME	SD
Nequip@ANI1x+D4	23.09 (23.70)	-23.09 (-23.70)	10.54 (10.37)
Nequip@SPICEv1	18.24 (17.89)	18.24 (17.89)	**9.12 (9.17)**
MACE-OFF23	9.02 (8.14)	5.56 (4.52)	9.54 (8.38)
MACE-MP-0+D3	13.81 (14.28)	-7.36 (-7.86)	15.98 (16.17)
MACE@SPICE2	**6.77 (5.18)**	**1.77 (-0.04)**	10.93 (7.00)
MatterSim+D4	20.42 (20.69)	-18.03 (-18.19)	19.44 (19.86)
orb-d3-v2	29.53 (30.86)	-26.26 (-27.47)	25.67 (25.60)
OMAT24eqV2_86M+D4	40.56 (37.76)	-33.02 (-29.87)	50.10 (48.95)
Nequip@OMDB+D4	12.31 (12.00)	10.47 (10.08)	10.01 (10.06)
PBE-MBD [47,27]	5.79	-3.86	4.82

can see that all UMLIPs have higher MAE and SD than PBE-MBD. The best performing UMLIP for lattice energy predictions according to MAE is MACE@SPICE2, followed by MACE-OFF23 and Nequip@OMDB+D4. OMAT24eqV2_86M+D4 and orb-d3-v2 show the largest errors and will not be considered further.

To the best of our knowledge, the only benchmark database of elastic properties of molecular crystals is the one of Spackman et al. [7] that provides experimentally determined elastic tensors [48–68] as well as their calculation with S-HF-3c. In order to compare results, our calculations were executed on the same dataset as with S-HF-3c in Ref. [7]. When multiple experimental results were reported for a single compound, the average was used for the comparison. We first compared predictions of the ensemble of Nequip@SPICE models and experiments in Fig. 3. Most of the predictions are within the distribution of values obtained with the ensemble. It should be noted, however, that the ensemble of models results in a rather wide spread of values. Detailed comparison for each crystal in the benchmark and each model in the ensemble of models is provided in Supplemental Material, Table S1. One can notice that not in all cases with all potentials our workflow finished with successful calculation and a reason is provided in the table.

Next, we turn to a comparison of experimental and quantum-mechanical calculations of elastic properties with predictions of studied

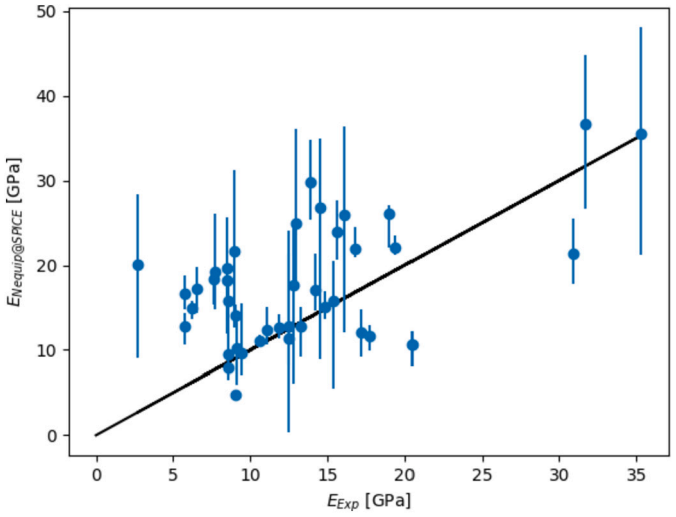

Fig. 3. Predictions of ensemble of Nequip@SPICE potential in comparison to Young's modulus obtained from experiments [7].

Table 3
MAE (and maximum error in parentheses) of the predictions for Young's modulus (E_{RH}) in GPa compared with the values from experiment, S-HF-3c and DFT-D calculations [7].

	Experiment	S-HF-3c	DFT-D
Nequip@ANI1x	9.97 (37.48)	7.42 (30.03)	5.97 (18.36)
Nequip@SPICEv1	7.05 (20.40)	4.83 (20.50)	5.61 (16.41)
Nequip@SPICEv2	6.86 (23.15)	4.93 (22.73)	5.76 (17.92)
Nequip@SPICEv3	7.43 (22.25)	6.48 (31.72)	4.22 (12.64)
Nequip@SPICEv4	7.77 (20.25)	**4.53** (20.69)	**3.19** (**8.07**)
Nequip@SPICEv5	6.97 (22.31)	5.96 (22.27)	4.63 (18.74)
Nequip@OMDB+D4	6.45 (23.50)	8.52 (18.94)	8.29 (15.97)
MACE-OFF23	6.78 (24.00)	**4.61** (**15.89**)	5.35 (16.60)
MACE-MP-0+D3	**5.51** (19.32)	6.01 (31.55)	4.75 (11.87)
MACE@SPICE2	7.14 (20.99)	**4.73** (20.10)	4.03 (14.25)
MatterSim+D4	**5.20** (**18.09**)	6.74 (24.63)	7.64 (21.68)
S-HF-3c	5.79 (17.58)	-	3.88 (14.46)
DFT-D	5.56 (14.45)	3.88 (14.46)	-

UMLIPs as shown in Table 3. All UMLIPs show reasonable agreement with experimental Young's modulus with MAEs in the range of 5–10 GPa. Importantly, MAE between experiments and S-HF-3c and DFT-D calculations is in the range of 5–6 GPa, the same as better performing UMLIPs. The agreement between UMLIPs and S-HF-3c and DFT-D calculations is somewhat better. The MAE of better-performing models compared to S-HF-3c and DFT-D is below 5 GPa. This is also expected as in both cases it is calculated in the same way while in experiments there are other effects, notably temperature. The best performance with respect to S-HF-3c and DFT-D calculations is provided with some of the Nequip@SPICE models, MACE-OFF23 and MACE@SPICE2, all trained on the SPICE dataset. MACE-MP-0+D3 and MatterSim+D4 also work well and have the lowest MAE compared to experiments. Table 3 also shows maximum absolute errors, which are all relatively high considering that their magnitude is even higher than the typical values of Young's modulus. In Fig. 4, we compare UMLIPs predictions for Young's modulus with S-HF-3c predictions and in Fig. 5 with experimental values. These figures show that there is a significant spread of predictions in comparison to S-HF-3c and experiments, but also between different UMLIPs. From the perspective of UMLIPs, it is rather comforting that DFT-D (PBEh3c) and S-HF-3c also show a similar spread of predictions with the tendency of overestimation in comparison to experiments, and also have significant spread between each other as can be seen in Fig. 5. Full details for each model and each crystal are given in Supplemental Material, Tables S1–S2. In the Supplemental Material, we have also

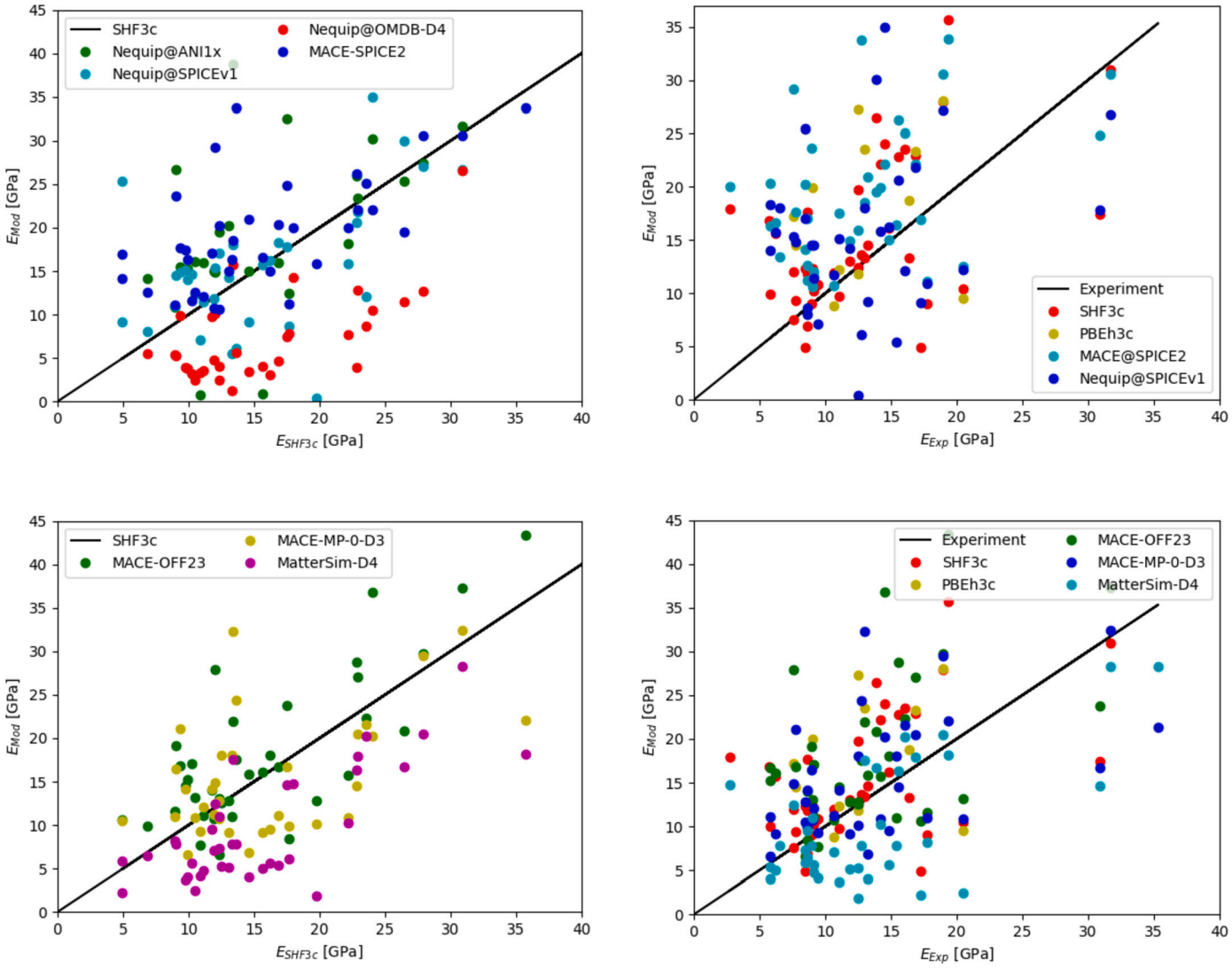

Fig. 4. Predictions of different UMLIPs in comparison to Young's modulus obtained from the S-HF-3c method.

Fig. 5. Young's modulus obtained with S-HF-3c [7], PBE3c [69–72] and different UMLIPs compared to experimental values.

compared UMLIPs predictions of universal anisotropy (Tables S3–S4) and Poisson's ratio (Tables S5-S6) to experimental values and S-HF-3c and DFT-D calculations. For universal anisotropy, the best performing models are Nequip@SPICEv4, Nequip@ANI1x and MACE-OFF23. For Poisson's ratio there is less difference between UMLIPs. The smallest MAEs compared to experiment and S-HF-3c calculations is obtained by Nequip@SPICEv4 and MACE@SPICE2. From here, we continue to work with Nequip@SPICE and MACE-OFF23 potentials as they have shown reasonable predictions of elastic properties and stability in calculations.

One of the peculiar properties is the occurrence of negative linear compressibility. In Fig. 6, we compare predictions of linear compressibility between quantum-mechanical predictions (S-HF-3c and PBEh3c) with four chosen UMLIPs (Nequip@SPICEv1, MACE-OFF23, MACE-MP-0+D3, and MatterSim+D4). Conclusions remain similar, predictions are reasonable but with a significant spread between methods. One can notice a somewhat better agreement between S-HF-3c and PBEh3c.

Once we have established the usefulness of UMLIPs for predictions of elastic properties of molecular crystals, we turn to the high-throughput screening of elastic properties (the stiffness tensor, elastic modulus constants, and linear compressibility) of molecular crystals. We have selected 8000 molecular crystals with the smallest unit cells that crystalize in needle-like from the CSD database [73]. The needle-like form was selected as such crystals are experimentally easier to characterize and more useful for applications. In Fig. 7 we show a histogram of predictions of Young's modulus using Nequip@SPICEv1. Most of the structures have Young's modulus in the range of 9–16 GPa. Similar distributions of Young's modulus are obtained with Nequip@SPICEv3 and MACE-OFF23 potentials (see Figs. S1 and S2). One should note that there is a significant spread in predictions between different versions of Nequip@SPICE models or between Nequip@SPICE and MACE-OFF23, as shown in Figs. S3 and S4. This points out to the relatively high uncertainty associated with predictions.

Of particular interest for applications are soft molecular crystals. We have identified around 40 structures with very low Young's modulus (0–2 GPa) predicted with Nequip@SPICEv1. The lowest Young's modulus was predicted for molecular crystals with the following CSD identifier: IQIHOI, GACCAS, BODSIZ, GEFXOI, MEWSAK, and SUFJEL. For these crystals, we have performed PBE-MBD DFT calculations to check the predictions. Fig. 8 shows a comparison of Nequip@SPICEv1 predictions for these six crystals and two typical crystals with predictions of PBE-MBD DFT and MACE-OFF23. For all six crystals for which Nequip@SPICEv1 predicted very low Young's modulus, PBE-MBD DFT predicts a much larger Young's modulus. Except for SUFJEL, MACE-OFF23 agrees with DFT showing that these predictions come from inaccuracies of Nequip@SPICEv1. For the two typical crystals (AMAFEZ and BZOXZO03) agreement between our DFT calculations and

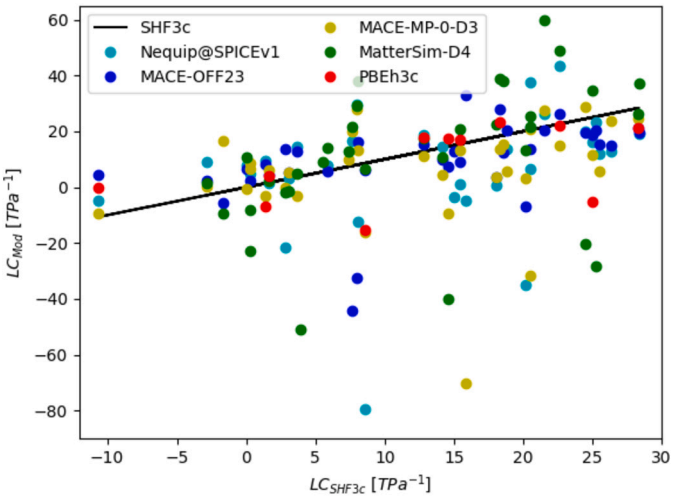

Fig. 6. Linear compressibility predictions of MACE-OFF23, Nequip@SPICEv1, and PBEh3c in comparison to S-HF-3c.

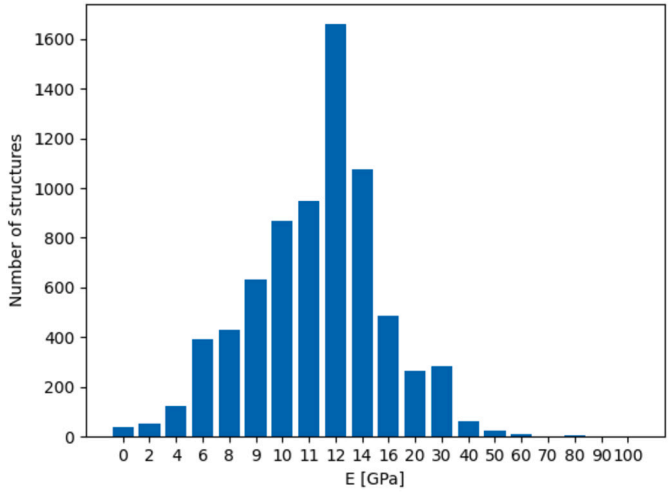

Fig. 7. Histogram of Young's modulus predictions by Nequip@SPICEv1 potential.

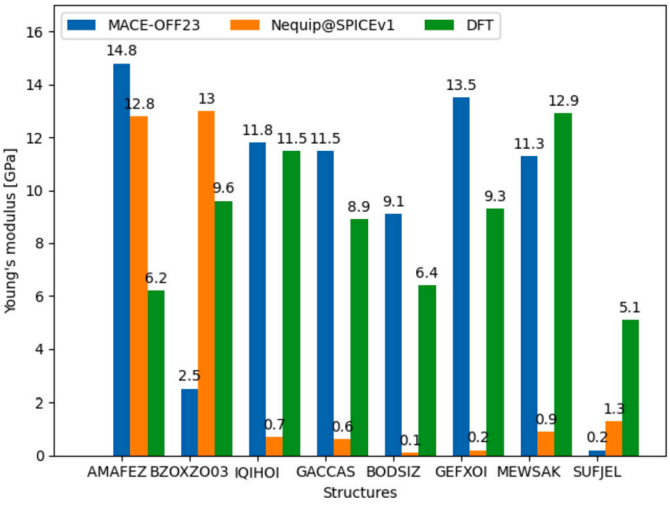

Fig. 8. Validation of Nequip@SPICEv1 predicted low Young's modulus crystals (IQIHOI, GACCAS, BODSIZ, GEFXOI, MEWSAK, SUFJEL) and typical crystals (AMAFEZ, BZOXZO03) with PBE-MBD DFT and MACE-OFF23.

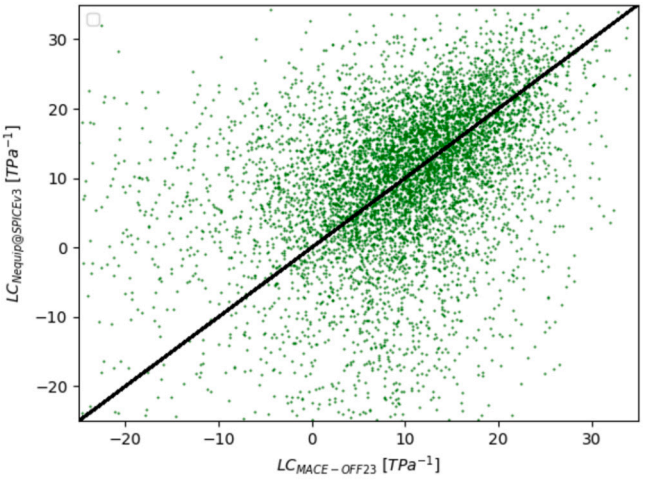

Fig. 9. Comparison of linear compressibility from high-throughput screening obtained by MACE-OFF23 and Nequip@SPICEv3 potentials.

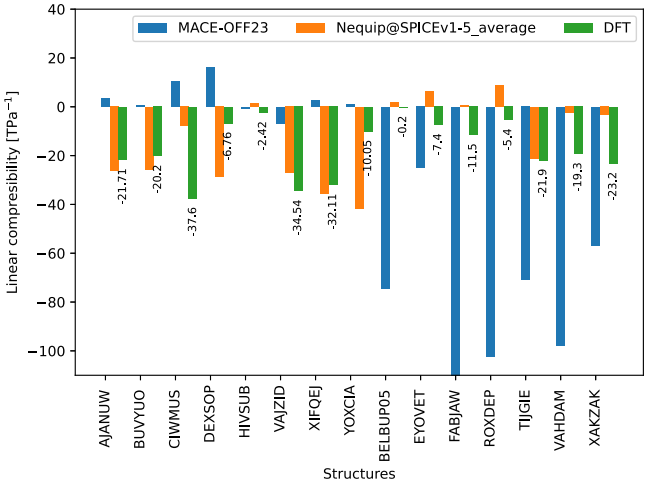

Fig. 10. Validation of prediction of negative linear compressibility. Comparison of results obtained by MACE-OFF23, average of Nequip@SPICE models, and PBE+MBD DFT.

Nequip@SPICEv1 is reasonable. This analysis also shows that for screening purposes, one should seek agreement between different potentials before the validation with DFT.

Next, we performed a high-throughput screening of linear compressibilities using the same 8000 needle-like crystals from CSD. We start by plotting a comparison of predictions of linear compressibilities for the MACE-OFF23 and Nequip@SPICEv3 potentials in Fig. 9. There is a clear correlation in predictions of the two potentials but, again, with a significant spread between the two. Most of the linear compressibilities lie in the range of 0–25 TPa^{-1}. As expected, negative linear compressibility is a rather rare phenomenon and, according to predictions of Nequip@SPICEv1, 14% of structures show negative linear compressibility.

We have selected several molecular crystals with negative linear compressibility according to Nequip@SPICEv1 potential that were also confirmed by Nequip@SPICEv3 potential, see Supplemental Material, Table S7. We then validated these predictions with PBE-MBD DFT calculations. We have found that for the structures with the following CSD identifiers AJANUW, BUVYUO, CIWMUS, DEXSOP, HIVSUB, VAJZIT, XIFQEJ, YOXCIA, BELBUP05, EYOVET, FABJAW, ROXDEP, TIJGIE, VAHDAM, and XAKZAK, PBE-MBD DFT confirmed the negative linear compressibility. A comparison of calculated linear compressibilities is shown in Fig. 10. PBE-MBD DFT predictions show strong negative

linear compressibility of $<$-10 TPa^{-1} for 10 structures that can be readily confirmed by experiments.

4. Discussion and conclusion

We have benchmarked existing and newly trained UMLIPs for predicting the properties of molecular crystals. Based on the X23b benchmark for volumes and lattice energies, we show that UMLIPs trained on the SPICE dataset, such as MACE@SPICE2 and MACE-OF23 provide good predictions approaching the accuracy of well-established DFT approximations such as PBE-MBD.

DFT-like accuracy of chosen UMLIPs is also transferred to predictions of elastic properties. However, predictions of DFT-based methods and methods such as S-HF-3c also come with significant differences compared to experimentally determined elastic constants. Typically, errors in predictions of Young's modulus compared to experiments are larger than 5 GPa. Similar errors are obtained when UMLIPs are compared to DFT or S-HF-3c. Significant differences between DFT-based methods and experiments point out to the need for methodological advances in simulations of elastic properties of materials. Such advances could include temperature effects to better represent experimental conditions. In this perspective, due to their speed, machine learning potentials are helpful. As can be seen in the Table S8, UMLIPs are around 3 orders of magnitude faster than DFT in elastic tensor calculation.

Keeping in mind these deficiencies, we have performed a high-throughput study of the elastic properties of needle-like molecular crystals which provides information on the typical and extremal elastic properties. According to our calculations, typical molecular crystals have Young's modulus of 9-16 GPa. We have identified some crystals with low modulus, which are interesting for applications, but DFT validation of these results showed that these were false results. A more complete screening is needed in this case, and it is desirable that more than one UMLIP agree in the prediction since we have shown that predictions come with significant uncertainty that is exemplified by the comparison of predictions of different versions of UMLIPs trained with the same architecture and dataset.

We have also searched for crystals with negative linear compressibility. We have identified several structures where different versions of our Nequip@SPICE UMLIP agree in the prediction of negative linear compressibility. The predictions were then also confirmed with PBE-MBD DFT that are ready to be experimentally verified.

CRediT authorship contribution statement

Anastasiia Kholtobina: Writing – original draft, Visualization, Formal analysis, Data curation. **Ivor Lončarić:** Writing – review & editing, Supervision, Software, Resources, Project administration, Methodology, Funding acquisition, Conceptualization.

Declaration of competing interest

The authors declare the following financial interests/personal relationships which may be considered as potential competing interests: Ivor Loncaric reports financial support was provided by Croatian Science Foundation. If there are other authors, they declare that they have no known competing financial interests or personal relationships that could have appeared to influence the work reported in this paper.

Acknowledgements

This work has been supported by Croatian Science Foundation under the project UIP-2020-02-5675.

Appendix A. Supplementary material

Supplementary material related to this article can be found online at https://doi.org/10.1016/j.matdes.2025.114047.

Data availability

Our machine learning models, calculation script and results of elastic calculations are openly available in Zenodo at https://doi.org/10.5281/zenodo.15225984.

References

[1] T.W. Ko, S.P. Ong, Recent advances and outstanding challenges for machine learning interatomic potentials, Nat. Comput. Sci. 3 (2023) 998.
[2] B. Mortazavi, Recent advances in machine learning-assisted multiscale design of energy materials, Adv. Energy Mater. 15 (2025) 2403876.
[3] J. Riebesell, R.E. Goodall, A. Jain, P. Benner, K.A. Persson, A.A. Lee, Matbench discovery–an evaluation framework for machine learning crystal stability prediction, arXiv preprint, arXiv:2308.14920, 2023.
[4] L. Catalano, D.P. Karothu, S. Schramm, E. Ahmed, R. Rezgui, T.J. Barber, A. Famulari, P. Naumov, Angew. Chem. 57 (2018) 17254–17258.
[5] S. Zhao, H. Yamagishi, O. Oki, Y. Ihara, N. Ichiji, A. Kubo, S. Hayashi, Y. Yamamoto, Adv. Opt. Mater. 10 (2022) 2101808.
[6] G.A. Dolgonos, J. Hoja, A.D. Boese, Revised values for the x23 benchmark set of molecular crystals, Phys. Chem. Chem. Phys. 21 (2019) 24333.
[7] P.R. Spackman, A. Grosjean, S.P. Thomas, D.P. Karothu, P. Naumov, M.A. Spackman, Quantifying mechanical properties of molecular crystals: a critical overview of experimental elastic tensors, Angew. Chem. Int. Ed. 61 (2022) e202110716.
[8] M. Brunsteiner, S. Nilsson-Lil, L.M. Morgan, A. Davis, A. Paudel, Finite-temperature mechanical properties of organic molecular crystals from classical molecular simulation, Cryst. Growth Des. 23 (2023) 2155–2168.
[9] I.A. Fedorov, C.V. Nguyen, A.Y. Prosekov, Study of the elastic properties of the energetic molecular crystals using density functionals with van der Waals corrections, ACS Omega 6 (2020) 642.
[10] M. Seehaus, S.-H. Lee, T. Stollenwerk, J.M. Wheeler, S. Korte-Kerzel, Estimation of directional single crystal elastic properties from nano-indentation by correlation with ebsd and first-principle calculations, Mater. Des. 234 (2023) 112296.
[11] T. Taniguchi, Exploration of elastic moduli of molecular crystals via database screening by pretrained neural network potential, CrystEngComm 24 (2024) 631.
[12] I. Batatia, et al., A foundation model for atomistic materials chemistry, arXiv:2401.00096 [physics.chem-ph], 2023.
[13] I. Batatia, D.P. Kovacs, G.N.C. Simm, C. Ortner, G. Csanyi, Mace: higher order equivariant message passing neural networks for fast and accurate force fields, Adv. Neural Inf. Process. Syst. (2022).
[14] B. Deng, P. Zhong, K. Jun, J. Riebesell, K. Han, C.J. Bartel, G. Ceder, Chgnet as a pretrained universal neural network potential for charge-informed atomistic modelling, Nat. Mach. Intell. 5 (2023) 1031.
[15] S. Grimme, J. Antony, S. Ehrlich, H. Krieg, A consistent and accurate ab initio parametrization of density functional dispersion correction (dft-d) for the 94 elements h-pu, J. Chem. Phys. 132 (2010).
[16] H. Yang, C. Hu, Y. Zhou, X. Liu, Y. Shi, J. Li, G. Li, Z. Chen, S. Chen, C. Zeni, M. Horton, R. Pinsler, A. Fowler, D. Zügner, T. Xie, J. Smith, L. Sun, Q. Wang, L. Kong, C. Liu, H. Hao, Z. Lu, Mattersim: a deep learning atomistic model across elements, temperatures and pressures, arXiv preprint, arXiv:2405.04967, 2024, arXiv:2405.04967 [cond-mat.mtrl-sci].
[17] C. Chen, S.P. Ong, A universal graph deep learning interatomic potential for the periodic table, Nat. Comput. Sci. 2 (2022) 718.
[18] E. Caldeweyher, J.-M. Mewes, S. Ehlert, S. Grimme, Extension and evaluation of the d4 London-dispersion model for periodic systems, Phys. Chem. Chem. Phys. 22 (2020) 8499.
[19] M. Neumann, J. Gin, B. Rhodes, S. Bennett, Z. Li, H. Choubisa, A. Hussey, J. Godwin, Orb: a fast, scalable neural network potential, arXiv:2410.22570 [cond-mat.mtrl-sci], 2024.
[20] A. Sanchez-Gonzalez, J. Godwin, T. Pfaff, R. Ying, J. Leskovec, P. Battaglia, Learning to simulate complex physics with graph networks, in: International Conference on Machine Learning, PMLR, 2020, pp. 8459–8468.
[21] J. Schmidt, L. Pettersson, C. Verdozzi, S. Botti, M.A. Marques, Crystal graph attention networks for the prediction of stable materials, Sci. Adv. 7 (2021) eabi7948.
[22] J. Schmidt, T.F. Cerqueira, A.H. Romero, A. Loew, F. Jäger, H.-C. Wang, S. Botti, M.A. Marques, Improving machine-learning models in materials science through large datasets, Mater. Today Phys. 48 (2024) 101560.
[23] L. Barroso-Luque, M. Shuaibi, X. Fu, B.M. Wood, M. Dzamba, M. Gao, A. Rizvi, C.L. Zitnick, Z.W. Ulissi, Open materials 2024 (omat24) inorganic materials dataset and models, arXiv preprint, arXiv:2410.12771, 2024.
[24] Y.-L. Liao, B. Wood, A. Das, T. Smidt, Equiformerv2: improved equivariant transformer for scaling to higher-degree representations, arXiv preprint, arXiv:2306.12059, 2023.
[25] D.P. Kovács, J.H. Moore, N.J. Browning, I. Batatia, J.T. Horton, V. Kapil, W.C. Witt, I.-B. Magdău, D.J. Cole, G. Csányi, Mace-off23: transferable machine learning force fields for organic molecules, arXiv preprint, arXiv:2312.15211, 2023.
[26] P. Eastman, P.K. Behara, D.L. Dotson, R. Galvelis, J.E. Herr, J.T. Horton, Y. Mao, J.D. Chodera, B.P. Pritchard, Y. Wang, et al., Spice, a dataset of drug-like molecules and peptides for training machine learning potentials, Sci. Data 10 (2023) 11.

[27] I. Žugec, R.M. Geilhufe, I. Lončarić, Global machine learning potentials for molecular crystals, J. Chem. Phys. 160 (2024).
[28] S. Batzner, A. Musaelian, L. Sun, M. Geiger, J.P. Mailoa, M. Kornbluth, N. Molinari, T.E. Smidt, B. Kozinsky, E(3)-equivariant graph neural networks for data-efficient and accurate interatomic potentials, Nat. Commun. 13 (2022) 2453.
[29] J.S. Smith, R. Zubatyuk, B. Nebgen, N. Lubbers, K. Barros, A.E. Roitberg, O. Isayev, S. Tretiak, The ani-1ccx and ani-1x data sets, coupled-cluster and density functional theory properties for molecules, Sci. Data 7 (2020) 134.
[30] S.S. Borysov, R.M. Geilhufe, A.V. Balatsky, Organic materials database: an open-access online database for data mining, PLoS ONE 12 (2017) 1.
[31] S.P. Ong, W.D. Richards, A. Jain, G. Hautier, M. Kocher, S. Cholia, D. Gunter, V.L. Chevrier, K.A. Persson, G. Ceder, Python materials genomics (pymatgen): a robust, open-source python library for materials analysis, Comput. Mater. Sci. 68 (2013) 314.
[32] R. Zhao, S. Wang, Z. Kong, Y. Xu, K. Fu, P. Peng, C. Wu, Development of a neuroevolution machine learning potential of pd-cu-ni-p alloys, Mater. Des. 231 (2023) 112012.
[33] B. Mukhamedov, F. Tasnadi, I.A. Abrikosov, Machine learning interatomic potential for the low-modulus ti-nb-zr alloys in the vicinity of dynamical instability, Mater. Des. 113865 (2025).
[34] J. Nye, Physical properties of crystals, 1985.
[35] R. Gaillac, P. Pullumbi, F.X. Coudert, J. Phys. Condens. Matter 28 (2016) 275201.
[36] V. Blum, R. Gehrke, F. Hanke, P. Havu, V. Havu, X. Ren, K. Reuter, M. Scheffler, Ab initio molecular simulations with numeric atom-centered orbitals, Comput. Phys. Commun. 180 (2009) 2175.
[37] F. Knuth, C. Carbogno, V. Atalla, V. Blum, M. Scheffler, All-electron formalism for total energy strain derivatives and stress tensor components for numeric atom-centered orbitals, Comput. Phys. Commun. 190 (2015) 33.
[38] V. Havu, V. Blum, P. Havu, M. Scheffler, Efficient o (n) integration for all-electron electronic structure calculation using numeric basis functions, J. Comput. Phys. 228 (2009) 8367.
[39] V. Blum, M. Rossi, S. Kokott, M. Scheffler, The fhi-aims code: all-electron, ab initio materials simulations towards the exascale, arXiv preprint, arXiv:2208.12335, 2022.
[40] J.P. Perdew, K. Burke, M. Ernzerhof, Generalized gradient approximation made simple, Phys. Rev. Lett. 77 (1996) 3865.
[41] A. Tkatchenko, R.A. DiStasio Jr., R. Car, M. Scheffler, Accurate and efficient method for many-body van der Waals interactions, Phys. Rev. Lett. 108 (2012) 236402.
[42] A. Ambrosetti, A.M. Reilly, R.A. DiStasio, A. Tkatchenko, Long-range correlation energy calculated from coupled atomic response functions, J. Chem. Phys. 140 (2014).
[43] A.M. Reilly, A. Tkatchenko, Role of dispersion interactions in the polymorphism and entropic stabilization of the aspirin crystal, Phys. Rev. Lett. 113 (2014) 055701.
[44] E. Kiely, R. Zwane, R. Fox, A.M. Reilly, S. Guerin, Density functional theory predictions of the mechanical properties of crystalline materials, CrystEngComm 23 (2021) 5697.
[45] K.M. Bal, A. Collas, Are elastic properties of molecular crystals within reach of density functional theory? Accuracy, robustness, and reproducibility of current approaches, Cryst. Growth Des. 24 (2024) 3714.
[46] J. Hoja, A.M. Reilly, A. Tkatchenko, First-principles modeling of molecular crystals: structures and stabilities, temperature and pressure, Wiley Interdiscip. Rev. Comput. Mol. Sci. 7 (2017) e1294.
[47] A.M. Reilly, A. Tkatchenko, Understanding the role of vibrations, exact exchange, and many-body van der Waals interactions in the cohesive properties of molecular crystals, J. Chem. Phys. 139 (2013).
[48] G. Afanaseva, K. Aleksandrov, A. Kitaigorodskii, Elastic constants of anthracene, Phys. Status Solidi 24 (1967) K61.
[49] V.V. Aleksandrov, K.N. Baransky, O.I. Vasileva, T.S. Velichkina, A.N. Izrailenko, I.A. Yakovlev, Opt. Spektrosk. 52 (1982) 193.
[50] A. Bain, N. El-Korashy, S. Gilmour, R. Pethrick, N.J. Sherwood, Ultrasonic and piezoelectric investigations on single crystals of 3-nitroaniline, Philos. Mag. B 66 (1992) 293.
[51] C. Bolme, K. Ramos, The elastic tensor of single crystal rdx determined by Brillouin spectroscopy, J. Appl. Phys. 116 (2014) 183503.
[52] L.-C. Brunel, Brillouin spectra and intermolecular potential of crystalline benzene, Chem. Phys. 37 (1979) 201.
[53] S. Chatterjee, S. Chakraborty, Elastic constants of acenaphthene determined from studies of thermal diffuse scattering of X-rays, Acta Crystallogr. Sect. A 37 (1981) 645.
[54] A. Chumakov, I. Silvestrova, K. Aleksandrov, Kristallografiya 3 (1958) 480.
[55] T. Danno, H. Inokuchi, Dynamic mechanical behaviour of organic molecular crystals. II. Elastic constants of single-crystal anthracene, Bull. Chem. Soc. Jpn. 41 (1968) 1783.
[56] R.C. Dye, C.J. Eckhardt, A complete set of elastic constants of crystalline anthracene by Brillouin scattering, J. Chem. Phys. 90 (1989) 2090.
[57] C. Ecolivet, M. Sanquer, K. Ishii, H. Nakayama, Ferroelasticity in phenothiazine: a Brillouin-scattering study, Phys. Rev. B 44 (1991) 4185.
[58] S. Haussühl, Z. Kristallogr. 216 (2001) 339.
[59] J.J. Haycraft, L.L. Stevens, C.J. Eckhardt, The elastic constants and related properties of the energetic material cyclotrimethylene trinitramine (rdx) determined by Brillouin scattering, J. Chem. Phys. 124 (2006) 024712.
[60] J.C.W. Heseltine, D.W. Elliott, O.B. Wilson, Elastic constants of single-crystal benzene, J. Chem. Phys. 40 (1964) 2584.
[61] H.B. Huntington, S.G. Gangoli, J.L. Mills, Ultrasonic measurement of the elastic constants of anthracene, J. Chem. Phys. 50 (1969) 3844.
[62] V. Koptsik, Kristallografiya 4 (1960) 197.
[63] J. Sapriel, R. Hierle, J. Zyss, M. Boissier, Acoustic and acousto-optic properties of 3-methyl 4-nitropyridine 1-oxide—a Brillouin scattering study, Appl. Phys. Lett. 55 (1989) 2594.
[64] C.J. Sartwell, J. Eckhardt, Brillouin-scattering study of the elastic constants of phenothiazine through the phase transition, Phys. Rev. B 48 (1993) 12438.
[65] R.B. Schwarz, D.E. Hooks, J.J. Dick, J.I. Archuleta, A.R. Martinez, Resonant ultrasound spectroscopy measurement of the elastic constants of cyclotrimethylene trinitramine, J. Appl. Phys. 98 (2005) 056106.
[66] C.J. Stevens, L.L. Eckhardt, The elastic constants and related properties of -hmx determined by Brillouin scattering, J. Chem. Phys. 122 (2005) 174701.
[67] B. Sun, J. Winey, Y. Gupta, D. Hooks, Determination of second-order elastic constants of cyclotetramethylene tetranitramine (b-hmx) using impulsive stimulated thermal scattering, J. Appl. Phys. 106 (2009) 053505.
[68] F. Teslenko, Kristallografiya 12 (1968) 946.
[69] L.M. LeBlanc, A. Otero-de-la Roza, E.R. Johnson, Cryst. Growth Des. 16 (2016) 6867–6873.
[70] B. Winkler, V. Milman, Cryst. Growth Des. 20 (2020) 206–213.
[71] Q. Peng, G. Wang, G.-R. Liu, S. Grimme, S. De, J. Phys. Chem. B 119 (2015) 5896–5903.
[72] F. Colmenero, Phys. Chem. Chem. Phys. 21 (2019) 2673–2690.
[73] C.R. Groom, I.J. Bruno, M.P. Lightfoot, S.C. Ward, The Cambridge structural database, Acta Crystallogr., Sect. B 72 (2016) 171.